

Optimisation of Heat Transfer in Corrugated Tube Using Taguchi Method

Abhishek Sharma¹, Deeno pawar²

¹M.Tech Scholar, Department of Mechanical Engineering, LNCT Bhopal,

²Prof., Department of Mechanical Engineering, LNCT Bhopal.

Abstract: Corrugated tubes are increasingly becoming more fascinating techniques for acquiring higher efficiency in heat exchangers to minimise costs. Hence, a 1 mm thick aluminum tube of six-start spiral corrugations and one smooth tube were modeled using configurations based on Ansys software package. In this study, the effects of geometric parameters on the heat transfer characteristic are investigated and optimized for the best overall thermal-hydraulic performance using Taguchi method. It is found that corrugation height have dominant influence on heat transfer characteristic with contribution ratios of 74.79% respectively while corrugation pitch has minor effects. As far as pressure drop and flow friction characteristic is concerned, corrugation height have also dominant influence on pressure drop and flow friction characteristic with contribution ratios of 71.24% and 65.12% respectively while corrugation pitch has minor effects. The optimal combination for SNR-TPC is determined as A3B2.

Keywords: heat exchangers, corrugation, Corrugated tubes, corrugation pitch, Taguchi method, thermal-hydraulic performance.

1. INTRODUCTION

Heat transfer augmentation is always an important matter of concern since the enhancement of heat transfer rate leads to increase the performance of system which is quite important in various heat transfer applications. Twisted tapes are well known heat transfer enhancement devices and several correlations of heat transfer and pressure drop have been developed for different types of twisted tapes. The enhancement of heat transfer is obtained by developing swirl flow of the tube side fluid, which gives high velocities near boundary and fluid mixing and consequently high heat transfer coefficient. In heat transfer systems equipped with twisted tapes, the heat transfer and pressure drop. Basically, three approaches are available yet to enhance the rate of heat transfer, active method, passive method and the compound method [1]. A power source is essential for the active, certain surface modifications or extension, and inserts or fluid additives are used in the passive method, while the compound method is a combination of the above two methods such as surface modification with fluid vibration [2].

The motivation behind this activity is the desire to obtain more effective heat exchangers and other industrial applications [3], with the major objectives being to provide energy, material, and economic savings for the users of heat transfer enhancement technology.

In heat exchangers, corrugation and other surface modifications are commonly used because they are very effective in the heat transfer enhancement; also it is appearing very interesting for practical applications because it is a technique that promotes secondary recirculation flow, by inducing non-axial velocity

components [4]. Recently, a swirl or helical flow pattern produced by employing surface modifications or any other passive technique for heat transfer enhancement is very interesting [5]. Also, Spiral corrugation increases heat transfer enhancement due to secondary flow swirls and surface curvatures pass by fluid layers, which also causes pressure losses [6].

The main reason for employing heat transfer enhanced techniques is for cutting costs as well as for practical purposes. The major roles of corrugations are for enhancing the secondary re-circulation flows, via induction of the component the radial velocities as well as the mixing of the flow layer. These techniques have been widely utilized in recent heat exchangers [7]. The outcome generated from the surface area modifications or the manipulations of heat transfers, which has been demonstrated to induce swirls or spirally flowing patterns has attracted increasing interests [8]. Additionally, corrugation enhances heat transfer owing to the existence of mixing fluids generated through separations and re-attachments [9].

2. LITERATURE REVIEW

Effect of twisted tape dimensions

Instead of full length twisted tape, Saha et al. (2001) used regularly spaced twisted tape. They investigated experimentally the effect of twist ratio, space ratio, tape width, phase angle on heat transfer and concluded that reduction in tape width gives poor heat transfer and higher than zero phase angle creates complexity in tape manufacturing rather than improving the heat transfer. Eiamsa-ard et al. (2006) conducted experiments with a twisted tape with twist ratio of 6–8 for a full length tape and free space ratio of 1, 2 and 3 for a regularly spaced twisted tape insert. They concluded that the heat transfer coefficient increases with decrease in twist ratio and space ratio. Eiamsa-ard et al. (2009) also investigated the effect of short length twisted tape insert. They used twisted tape with fix twist ratio and different length ratio. Short length inserts generated strong swirl at the tube entrance while the full length tape produced strong swirl flow over the entire length. Outcome of their research revealed that the maximum Thermal Performance Factor obtained for full length tape is 1.04 at $Re = 4000$ and decreases as the length ratio decreases.

Sarada et al. (2011) observed that the width of the twisted tape significantly affects the heat transfer rate. It was found that the heat transfer enhances as the width of insert increases.

Piriyarungrod et al. (2015) presented the effect of taper in the twisted tape to enhance the heat transfer performance. Their experiments for different taper angles revealed that the taper twisted tape does not achieve the thermal performance factor more than 1.05 but increases the heat transfer rate. Thus, taper tape is not a feasible method for heat transfer enhancement.

Esmailzadeh et al. (2014) also analyzed the effect of thickness of twisted tape with nanofluid and showed that the increase in thickness of the tape increases the heat transfer rate, friction factor and TPF.

Eiamsa and Promvonge (2010) assessed the performance of alternate clockwise and counter clockwise twisted tape inserts. They used tapes in experiments having twist ratios of 3,4 and 5 each with three twist angles of 30° , 60° and 90° and conclude that the heat transfer rate and TPF of alternate twisted tapes are

higher than typical twisted tapes at similar operating conditions. Heat transfer rate and TPF (1.3–1.4) increase with decrease in twist ratio and increase in phase angle.

Effect of twist ratio

Patil and Vijaybabu (2012, 2014) conducted experiments to understand the effect of the twist ratio on heat transfer augmentation. They concluded that the heat transfer increases with decrease in twist ratio. Also the use of twisted tape in laminar flow can result in energy saving. Twisted tape with increasing–decreasing twist ratio (Fig. 1) has a TPF of 1.98–1.60 at low $Re = 100$ (Patil & Vijaybabu, 2014). Eiamsa-ard et al. (2012) employed sequentially, repeatedly and intermittently twisted tape with increasing decreasing twist ratios. Among the tapes tested, the repeatedly increasing-decreasing twist ratios offered the maximum TPF of around 1.03.

Effect of helical insert

Helical twisted tapes have also been used to enhance the heat transfer rate (Sivashanmugam & Suresh, 2007; Sivashanmugam & Nagarajan, 2007). These authors used the full length helical inserts with different twist ratios (Fig. 2), with equal and unequal lengths with right and left turns. Their experiments showed that the helical tape insert improves the heat transfer compared to a plain tube and the TPF with right-left helical insert could be obtained an up to 3 for different configurations.

Moawed (2011) used the helical screw tape inserts in an elliptical tube. For low Re , it was found that the maximum TPF of 1.2 could be obtained with a combination of pitch ratio of 1 and twist ratio of 0.22.

3. RESEARCH METHODOLOGY

Corrugated tubes are increasingly becoming more fascinating techniques for acquiring higher efficiency in heat exchangers to minimise costs [12]. Hence, a 1 mm thick aluminum tube of six-start spiral corrugations and one smooth tube were modeled using configurations based on Ansys software package. The primary corrugation parameters are the corrugation height (e) and corrugation pitch (p). The envelope diameter D_{en} of the tubes vary depending on corrugation heights e , and fixed bore diameter D_b of 13 mm, as presented in Fig. 3.1. For the 5 tubes used, each having classical parameters of spiral corrugations with heights to diameter e/D_n , spiral corrugations with pitch to diameter p/D_n and severity index $\phi = e^2/(pD_n)$

The Taguchi method is the commonly adopted approach for optimizing design parameters.

Table 3.1: The parameters and their values corresponding to their levels

Parameters	Level		
	I	II	III
corrugation height, e	2	4	6
corrugation pitch, p	20	14	11

Note: all dimensions in millimetre

Simulation runs corresponding to their values of each level

Simulation runs	Corrugation height, e	Corrugation pitch, p
1	2	20
2	2	14
3	2	10
4	4	20
5	4	14
6	4	10
7	6	20
8	6	14
9	6	10

4. RESULTS AND DISCUSSION

The differences in temperature was attributed to the mixing of fluid layers at the secondary region induced by corrugation, and as the corrugation becomes severe, the mixing will also increase.

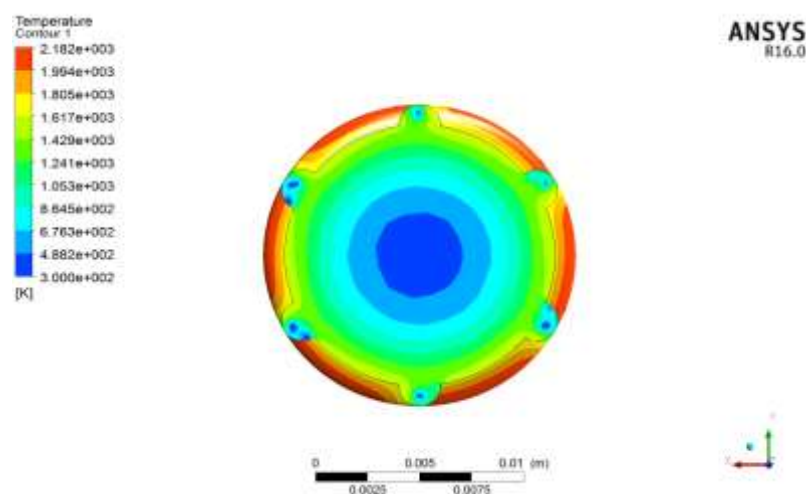


Fig. 4.1: Temperature contour for roughness height, $e = 2$ mm and pitch of corrugation, $p = 20$ mm

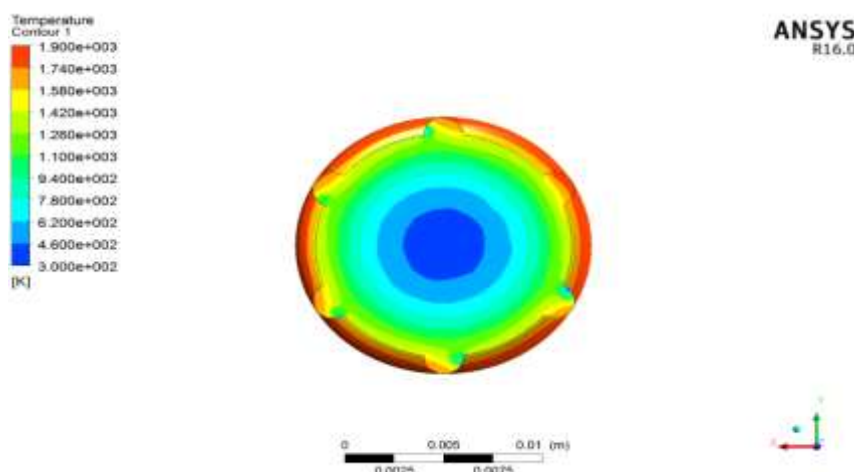


Fig. 4.2: Temperature contour for roughness height, $e = 2$ mm and Pitch of Corrugation, $p = 14$ mm

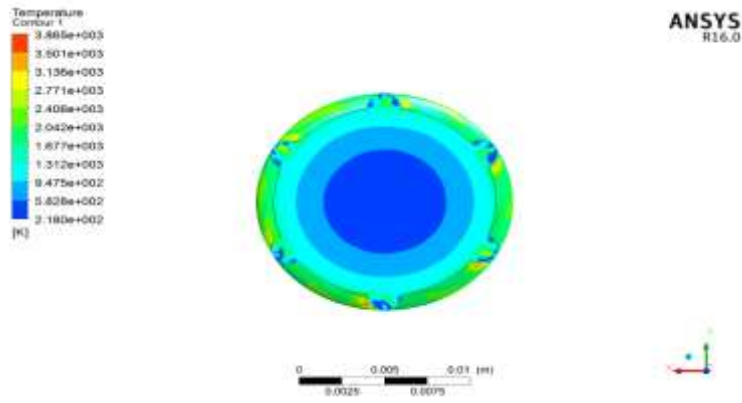


Fig. 4.3: Temperature contour for roughness height, $e = 2$ mm and Pitch of Corrugation, $p = 10$ mm

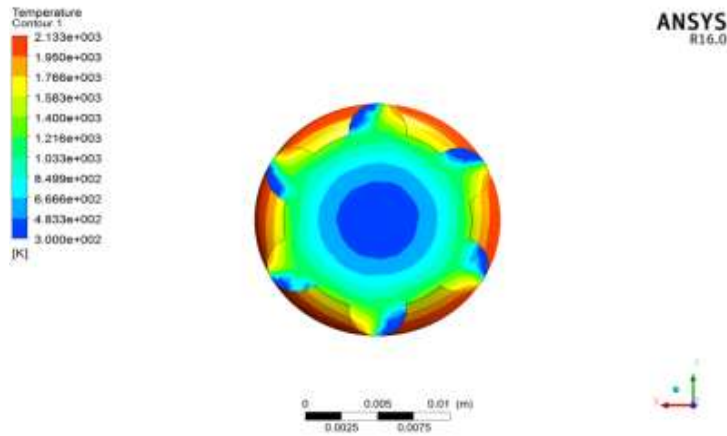


Fig. 4.4: Temperature contour for roughness height, $e = 4$ mm and Pitch of Corrugation, $p = 20$ mm

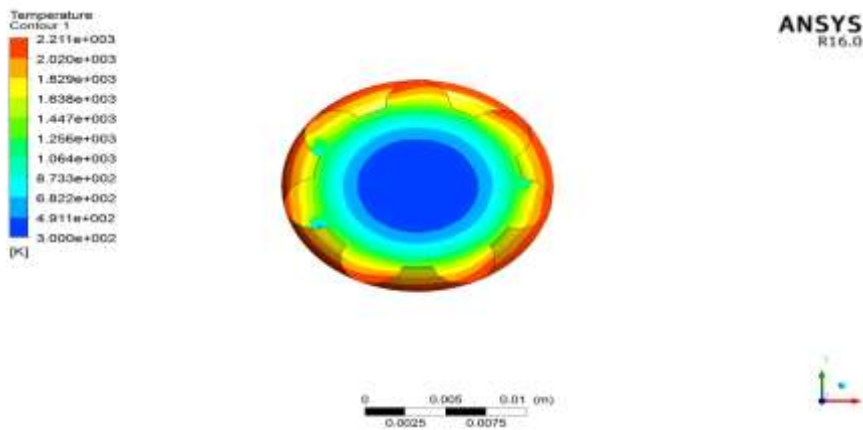


Fig. 4.5: Temperature contour for roughness height, $e = 4$ mm and Pitch of Corrugation, $p = 14$ mm

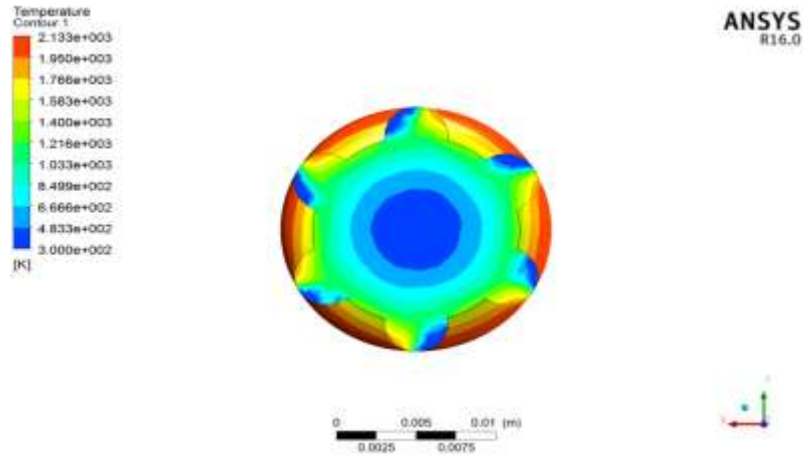


Fig. 4.6: Temperature contour for roughness height, $e = 4$ mm and Pitch of Corrugation, $p = 10$ mm

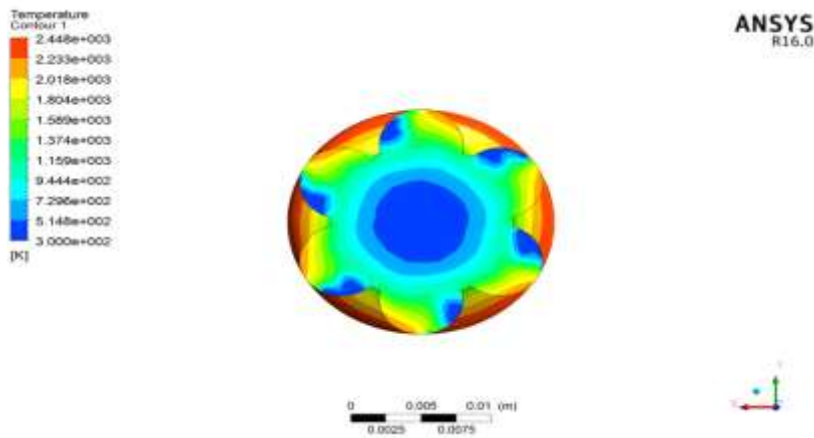


Fig. 4.7: Temperature contour for roughness height, $e = 6$ mm and Pitch of Corrugation, $p = 20$ mm

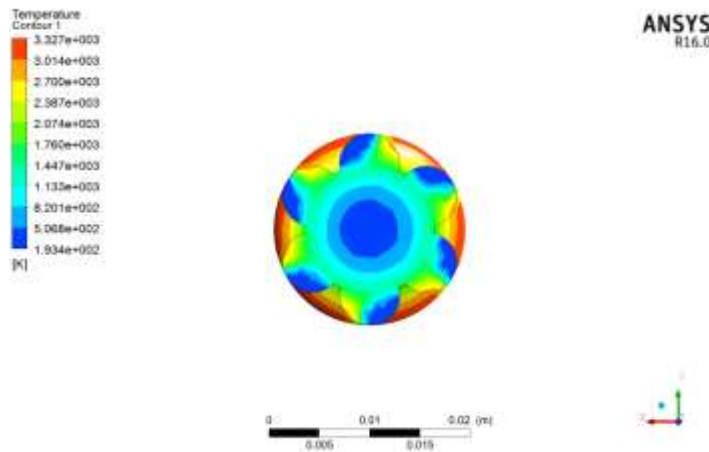


Fig. 4.8: Temperature contour for roughness height, $e = 6$ mm and Pitch of Corrugation, $p = 14$ mm

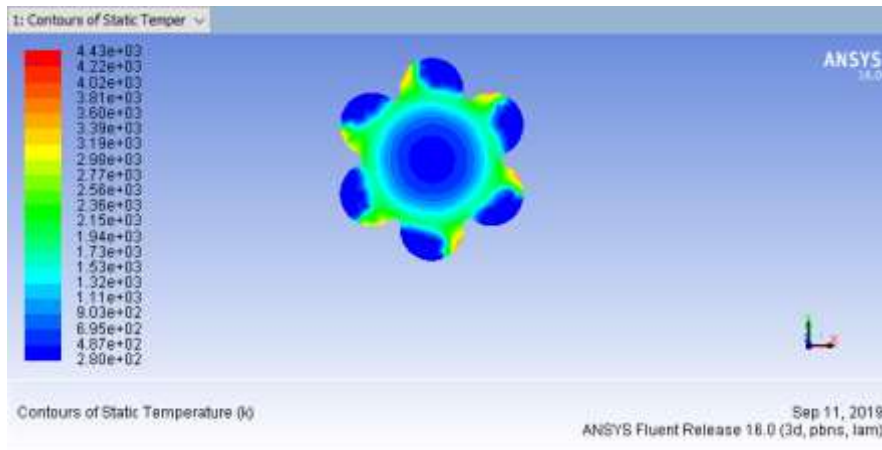


Fig. 4.9: Temperature contour for roughness height, $e = 6$ mm and Pitch of Corrugation, $p = 10$ mm

Table 4.1: Results of Nusselt number with nine simulation runs

For a heat exchanger, Nu describes the heat transfer characteristics. It is very important and helpful to know the influence of each factor on them when designing and optimizing a heat exchanger with surface roughness height and corrugation pitch. Based on table 4.3 contribution ratio of each factor are further presented in fig. 4.3.

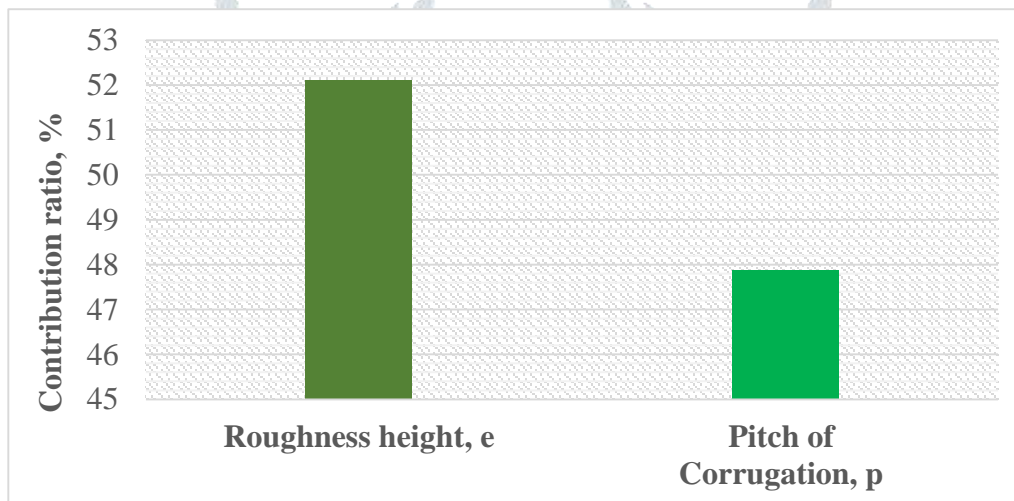


Fig. 4.10: Contribution ratio of factor towards Nu

The corresponding main-effect plots are also drawn to illustrate the effects of control factors according to the calculated average SNRs of each factor. Main-effect plots for SNR-Nu are shown in Fig. 4.11.

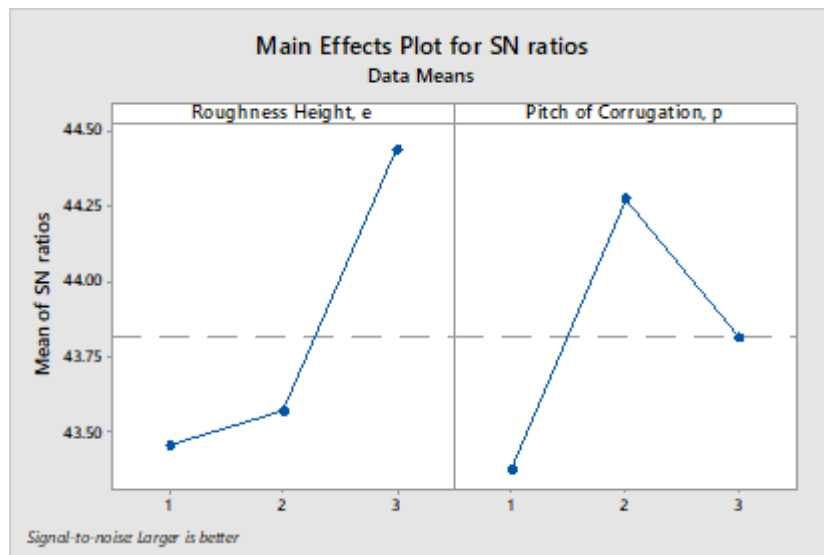


Fig. 4.11: Main-effect plots for SNR-Nu

From Fig. 4.11, it can be seen that the order of the parametric effectiveness for Nu is $e > p$. From fig. 4.11, the optimal combination for SNR-Nu is determined as A3B2. Based on table 4.5 contribution ratio of each factor are further presented in fig. 4.12.

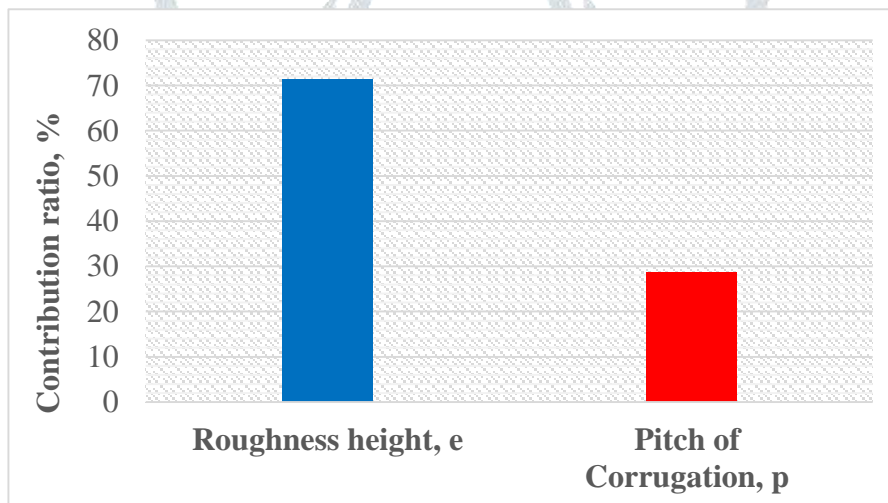


Fig. 4.12: Contribution ratio of factor towards pressure drop

The corresponding main-effect plots are also drawn to illustrate the effects of control factors according to the calculated average SNRs of each factor. Main-effect plots for SNR-P are shown in Fig. 4.13.

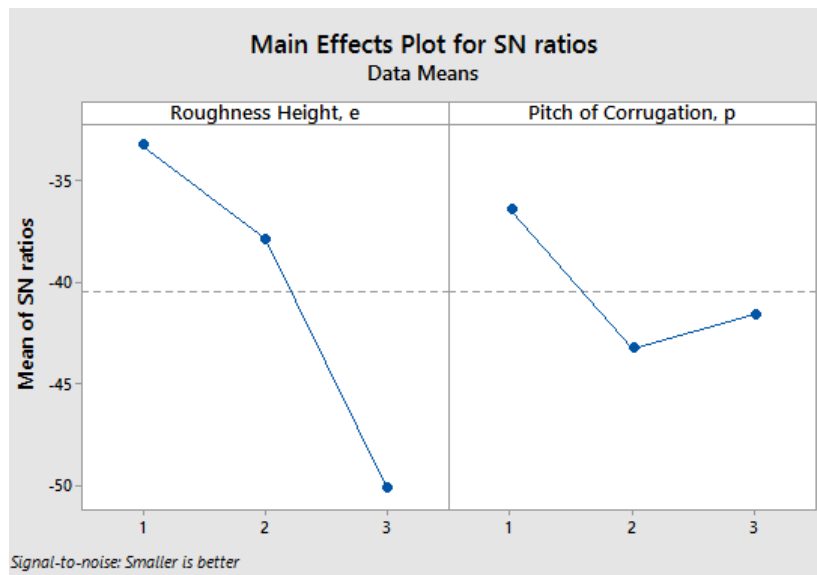


Fig. 4.13: Main-effect plots for SNR-Pressure drop

It has been known that the level that has the smallest SNR is the optimal level for the factor. If interaction effects between two factors can be negligible, the combinations of levels showing the largest SNR-P for each factor are regarded as the optimal level combination for pressure drop. From Fig. 4.13, it can be seen that the order of the parametric effectiveness for min. pressure drop is $e > p$. From fig. 4.13, the optimal combination for SNR-P is determined as A3B2.

4.3 FRICTION FACTOR RESULTS

contribution ratio of each factor are further presented in fig. 4.14.

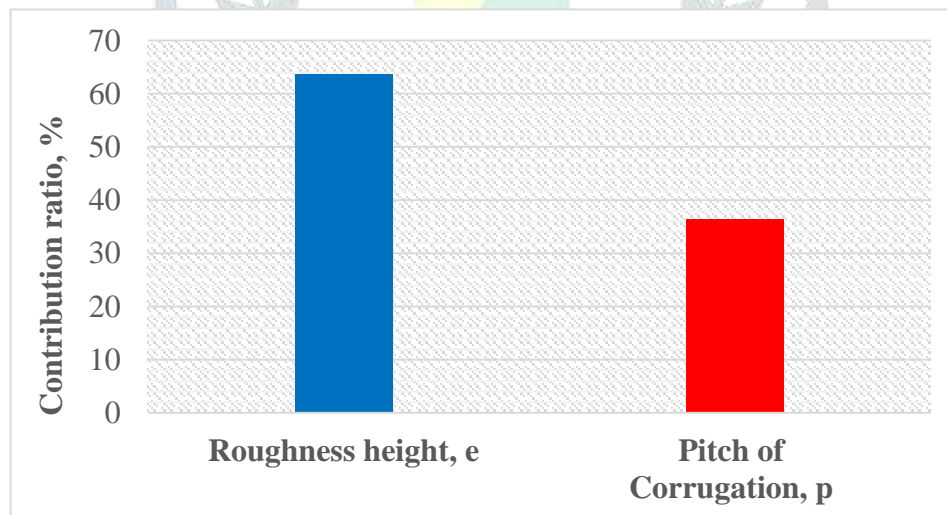


Fig. 4.14: Contribution ratio of factor towards pressure drop

The corresponding main-effect plots are also drawn to illustrate the effects of control factors according to the calculated average SNRs of each factor. Main-effect plots for SNR-f are shown in Fig. 4.14.

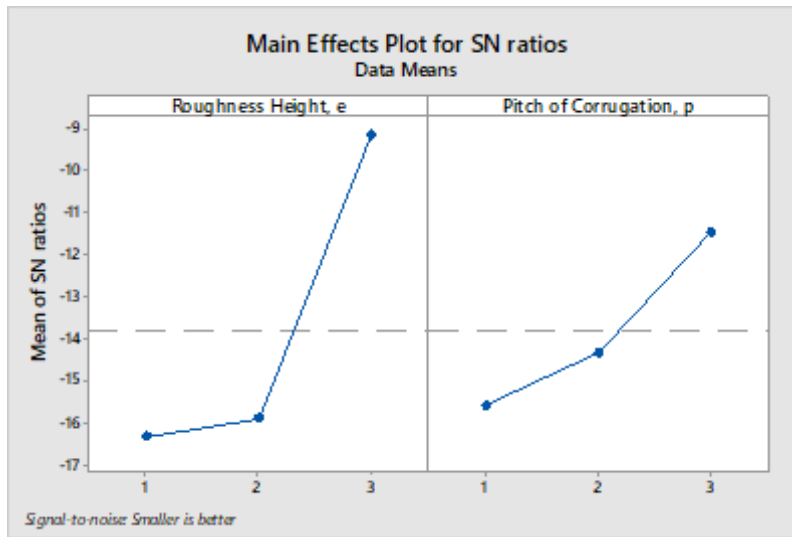


Fig. 4.15: Main-effect plots for SNR-friction factor

It has been known that the level that has the smallest SNR is the optimal level for the factor. If interaction effects between two factors can be negligible, the combinations of levels showing the largest SNR-f for each factor are regarded as the optimal level combination for friction factor. From Fig. 4.14, it can be seen that the order of the parametric effectiveness for min. pressure drop is $e > p$. From fig. 4.15, the optimal combination for SNR-f is determined as A3B3.

4.4 THERMAL PERFORMANCE CRITERIA RESULTS

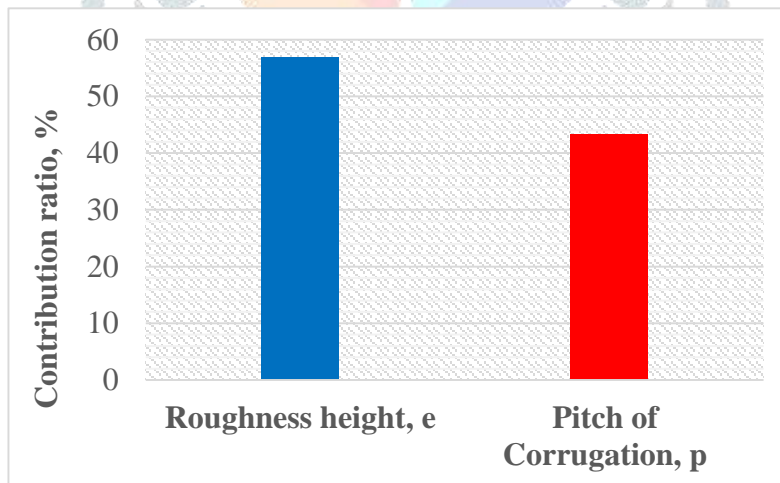


Fig. 4.16: Contribution ratio of factor towards TPC

The corresponding main-effect plots are also drawn to illustrate the effects of control factors according to the calculated average SNRs of each factor. Main-effect plots for SNR-TPC are shown in Fig. 4.17.

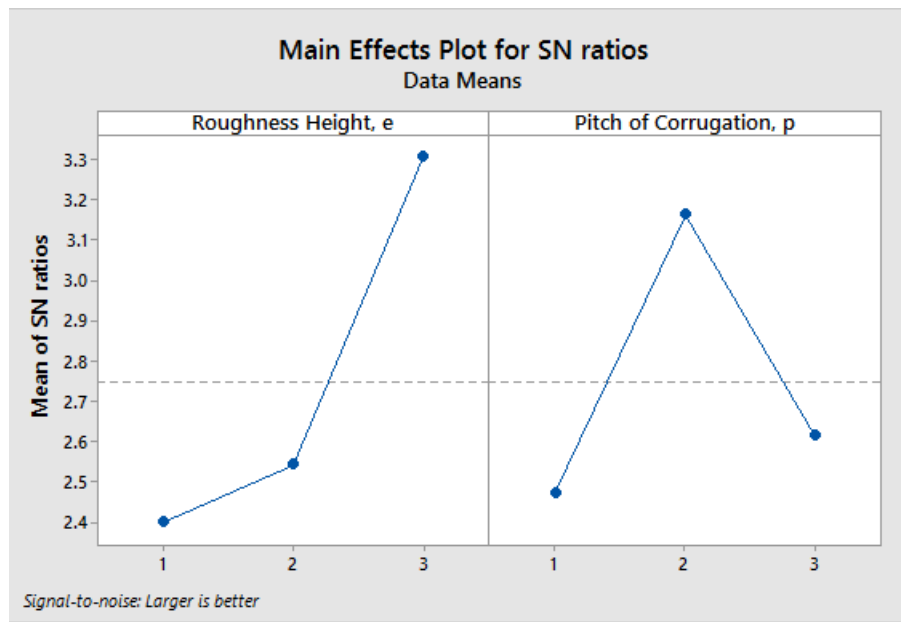


Fig. 4.17: Main-effect plots for SNR-TPC

It has been known that the level that has the smallest SNR is the optimal level for the factor. If interaction effects between two factors can be negligible, the combinations of levels showing the largest SNR-TPC for each factor are regarded as the optimal level combination for TPC. From Fig. 4.16, it can be seen that the order of the parametric effectiveness for max. TPC is $e > p$. From fig. 4.17, the optimal combination for SNR-TPC is determined as A3B2.

4. CONCLUSION

The main conclusions are drawn as follows:

1. The geometric parameters considered in the model include corrugation height and corrugation pitch. The results show that corrugation height have dominant influence on heat transfer characteristic with contribution ratios of 74.79% respectively while corrugation pitch has minor effects.
2. As far as pressure drop and flow friction characteristic is concerned, corrugation height have also dominant influence on pressure drop and flow friction characteristic with contribution ratios of 71.24% and 64.12% respectively while corrugation pitch has minor effects.
3. The effects of corrugation height and corrugation pitch on overall thermal-hydraulic performance are investigated. The results show that the corrugation height have dominant influence on heat transfer characteristic with contribution ratios of 56.77 % respectively while corrugation pitch has minor effects.
4. The optimal combination for SNR-TPC is determined as A3B2
5. The optimal combination for SNR-f is determined as A3B3
6. The optimal combination for SNR-P is determined as A3B2
7. The optimal combination for SNR-Nu is determined as A3B2

REFERENCES

- [1.] Saha, S.K., Dutta, A., Dhal, S.K., 2001. Friction and heat transfer characteristics of laminar swirl flow through a circular tube fitted with regularly spaced twisted tape elements. *Int. J. Heat Mass Transf.* 44 (22), 4211–4223.
- [2.] Eiamsa-ard, S., Thianpong, C., Promvonge, P., 2006. Experimental investigation of heat transfer and flow friction in a circular tube fitted with regularly spaced twisted tape elements. *Int. Commun. Heat Mass Transfer* 33 (10), 1225–1233.
- [3.] Eiamsa-ard, S. et al., 2009. Convective heat transfer in a circular tube with shortlength twisted tape insert. *Int. Commun. Heat Mass Transfer* 36 (4), 365–371.
- [4.] Sarada, S.N. et al., 2011. Enhancement of heat transfer using varying width twisted tape inserts. *Int. J. Eng., Sci. Technol.* 2 (6), 107–118.
- [5.] Piriyarungrod, N. et al., 2014. Heat transfer enhancement by tapered twisted tape inserts. *Chem. Eng. Process.* 96, 62–71.
- [6.] Esmaeilzadeh, E. et al., 2014. Study on heat transfer and friction factor characteristics of c-Al₂O₃/water through circular tube with twisted tape inserts with different thicknesses. *Int. J. Therm. Sci.* 82, 72–83.
- [7.] Eiamsa-ard, S., Promvonge, P., 2010. Performance assessment in a heat exchanger tube with alternate clockwise and counter-clockwise twisted-tape inserts. *Int. J. Heat Mass Transf.* 53 (7–8), 1364–1372.
- [8.] Patil, S.V., Babu, P.V.V., 2014. Heat transfer and pressure drop studies through a square duct fitted with increasing and decreasing order of twisted tape. *Heat Transfer Eng.* 35 (14–15), 1380–1387.
- [9.] Patil, S.V., Vijaybabu, P.V., 2012. Heat transfer enhancement through a square duct fitted with twisted tape inserts. *Heat and Mass Transfer/Waerme- und Stoffuebertragung* 48 (10), 1803–1811.
- [10.] Eiamsa-ard, S., Wongcharee, K., Promvonge, P., 2012b. Influence of nonuniform twisted tape on heat transfer enhancement characteristics. *Chem. Eng. Commun.* 199 (10), 1279–1297.
- [11.] Sivashanmugam, P., Nagarajan, P.K., 2007. Studies on heat transfer and friction factor characteristics of laminar flow through a circular tube fitted with right and left helical screw-tape inserts. *Exp. Thermal Fluid Sci.* 32 (1), 192–197.
- [12.] Sivashanmugam, P., Suresh, S., 2007. Experimental studies on heat transfer and friction factor characteristics of turbulent flow through a circular tube fitted with regularly spaced helical screw-tape inserts. *Appl. Therm. Eng.* 27 (8–9), 1311–1319.
- [13.] Moawed, M., 2011. Heat transfer and friction factor inside elliptic tubes fitted with helical screw-tape inserts. *J. Renewable Sustain. Energy* 3 (2), 23110.
- [14.] Bhuiya, M.M.K. et al., 2012. Heat transfer enhancement and development of correlation for turbulent flow through a tube with triple helical tape inserts. *Int. Commun. Heat Mass Transfer* 39 (1), 94–101.
- [15.] El Maakoul, A. et al., 2017. Numerical design and investigation of heat transfer enhancement and performance for an annulus with continuous helical baffles in a double-pipe heat exchanger. *Energy Convers. Manage.* 133, 76–86.

- [16.] Rahimi, M., Shabaniyan, S.R., Alsairafi, A.A., 2009. Experimental and CFD studies on heat transfer and friction factor characteristics of a tube equipped with modified twisted tape inserts. *Chem. Eng. Process.* 48 (3), 762–770.
- [17.] Shabaniyan, S.R. et al., 2011. CFD and experimental studies on heat transfer enhancement in an air cooler equipped with different tube inserts. *Int. Commun. Heat Mass Transfer* 38 (3), 383–390.
- [18.] Eiamsa-ard, S., Wongcharee, K., Eiamsa-ard, P., et al., 2010a. Heat transfer enhancement in a tube using delta-winglet twisted tape inserts. *Appl. Therm. Eng.* 30 (4), 310–318.
- [19.] Eiamsa-ard, S. et al., 2013a. Thermal performance evaluation of heat exchanger tubes equipped with coupling twisted tapes. *Exp. Heat Transf.* 26 (5), 413–430.
- [20.] Eiamsa-ard, S., Nuntadusit, C., Promvongse, P., 2013b. Effect of twin delta-winged twisted-tape on thermal performance of heat exchanger tube. *Heat Transfer Eng.* 34 (15), 1278–1288.
- [21.] Deshmukh, P.W., Vedula, R.P., 2014. Heat transfer and friction factor characteristics of turbulent flow through a circular tube fitted with vortex generator inserts. *Int. J. Heat Mass Transf.* 79, 551–560.
- [22.] Behfard, M., Sohankar, A., 2016. Numerical investigation for finding the appropriate design parameters of a fin-and-tube heat exchanger with delta-winglet vortex generators. *Heat Mass Transf.* 52 (1), 21–37.
- [23.] Nanan, K., Pimsarn, M., et al., 2013a. Heat transfer augmentation through the use of wire-rod bundles under constant wall heat flux condition. *Int. Commun. Heat Mass Transfer* 48, 133–140.
- [24.] Promvongse, P. et al., 2014. Experimental study on heat transfer in square duct with combined twisted-tape and winglet vortex generators. *Int. Commun. Heat Mass Transfer* 59, 158–164.
- [25.] Arulprakasajothi, M. et al., 2014. Experimental investigation on heat transfer effect of conical strip inserts in a circular tube under laminar flow. *Front Energy.*